The Astrophysical Journal, 635:950–958, 2005 December 20

COMPLETING THE COUNTS OF RADIO SOURCES AT 8.5 GHz

B. Henkel and R. B. Partridge
Department of Astronomy, Haverford College, Haverford, PA 19041;
brook.henkel@gmail.com, bpartrid@haverford.edu
Received 2005 July 1; accepted 2005 August 25

ABSTRACT

Most currently available counts of radio sources at frequencies >5 GHz are restricted to relatively bright sources. Observations made at NRAO's VLA have, however, provided counts of very *faint* sources ($S \lesssim 1$ mJy) at 8.5 GHz. Here we extend the 8.5 GHz VLA source counts to higher flux densities using both archival data and a brief, blind VLA survey at 8.5 GHz. We thus link the faint source counts to earlier source counts at $S \gtrsim 30$ mJy. The new counts of radio sources at 8.5 GHz hold no surprises.

Subject headings: cosmology: observations — radio continuum: galaxies

1. INTRODUCTION

Counts of extragalactic sources at radio wavelengths have long been used to explore the nature and evolution of radio sources (see Ryle 1968; Jauncey 1975; Condon 1992; Jackson & Wall 1999; Windhorst 2003) and thus to probe cosmological questions. Radio source counts have also established the emergence of new classes of radio sources, distinct from classical radio galaxies (Fomalont et al. 1984; Windhorst et al. 1985; Danese et al. 1987; see also reviews by Condon 1992; Windhorst 2003). Counts at 1.4 and 4.8 GHz were used by Haarsma et al. (2000) to measure the star formation history of the universe unaffected by dust extinction. We note that establishing the existence and properties of new classes of radio sources is made easier if counts at several frequencies are available, so that the average spectral indices and other properties of the sources can be determined.

Having multifrequency counts is even more crucial to a second and increasingly important use for radio source counts: modeling the foreground noise that extragalactic radio sources introduce into images of the cosmic microwave background, or CMB (see Toffolatti et al. 1998; Mason et al. 2003; De Zotti et al. 2005). Since most CMB observations are made at frequencies >20 GHz, counts at high frequencies, say above 5 GHz, are particularly important. Sources at 50–80 mJy and above, for instance, are expected to produce fluctuations $\gtrsim$5 times the receiver noise in the low-frequency channels of ESA's *Planck* mission at 30 and 44 GHz. Sources at 200–300 mJy are expected (Vielva et al. 2003) to be individually detectable in the *Planck* images at these frequencies.

Unfortunately, with the exception of two recently completed surveys of limited sky regions, source counts at frequencies above 5 GHz are quite fragmentary. The exceptions just mentioned are the 9C survey of Waldram et al. (2003), made at 15 GHz, and a southern survey being carried out at the Australia telescope at 16–20 GHz (Ricci et al. 2004). These surveys are restricted to relatively bright sources, with flux limits (to completeness) of 25 and $\sim$80 mJy, respectively. In addition, many of the experiments designed to detect fluctuations in the CMB are producing, as a by-product, catalogs of bright sources. These include surveys conducted by the DASI (Degree Angular Scale Interferometer) team (Kovac et al. 2002), the CBI (Cosmic Background Imager) team (Mason et al. 2003), and most recently *WMAP* (*Wilkinson Microwave Anisotropy Probe*; Bennett et al. 2003). The first two surveys were conducted over limited areas of the sky at 30 GHz, reaching 100 and $\sim$5 mJy, respectively. The *WMAP* satellite completed an all-sky survey, of course, but its counts were limited to $S \gtrsim 1$ Jy at $\nu = 22-90$ GHz. NRAO's Very Large Array (VLA)[1] has been used to make 8.5 GHz counts at very *low* flux densities ($S \lesssim 1$ mJy; Fomalont et al. 1997, 2002), but over very small regions of the sky. There is some evidence of variation in the faint source counts from region to region (see Fomalont et al. 2002). Finally, there are a few counts of very bright sources at 10 GHz made some years ago by Aizu et al. (1987). The counts by Aizu et al. are not truly unbiased, since these workers observed at 10 GHz sources *already detected* at a lower frequency of 5 GHz. What are missing are *systematic* counts at $\nu > 5$ GHz over the flux interval 0.3–30 mJy and an unbiased survey at $S > 0.3$ mJy.

The difficulty of making high-frequency, large-area surveys that reach mJy sensitivities is easily illustrated by calculating the observing time needed to reach a survey flux density limit S over a given solid angle Ω. If we assume that the detector sensitivity expressed in receiver temperature $T_{\rm rec}$ is independent of frequency, then the integrating time is easily shown to be given by

$$t \propto \left(\frac{T_{\rm rec}}{S}\right)^2 \frac{\nu^4}{\Delta\nu} \Omega\Omega_A,$$

or $\propto \nu^4$ for fixed S and Ω, where $\Delta\nu$ is the receiver bandwidth and Ω_A is the antenna beam solid angle. For a (diffraction-limited) antenna of fixed size, $\Omega_A \propto \nu^{-2}$, which makes $t \propto \nu^2$ in that case. In fact, the assumption that receiver temperature is independent of frequency is optimistic; in general, higher frequency receivers have higher noise temperatures, making them less sensitive. In addition, the quick calculation above ignored the slew time needed to move from one survey area to another. Alternatively, we can consider the time needed to detect a statistically significant sample of N sources. If we make the simple assumption that sources are randomly distributed in Euclidean space, then the integral count of sources brighter than S per steradian $N(>S)$ varies as $S^{-3/2}$, and the solid angle required to detect N sources is $\Omega \propto N^{-1}$. It follows that $t \propto S^{-1/2}$ for the detection of a fixed number of sources. Thus, shallow surveys are quicker, explaining why the 9C (Waldram et al. 2003) and

[1] The National Radio Astronomy Observatory is a facility of the National Science Foundation operated under cooperative agreement by Associated Universities, Inc.

ATCA (Australia Telescope Compact Array; Ricci et al. 2004) surveys are relatively shallow. As another illustration, the deep 8.5 GHz VLA surveys of Fomalont et al. (1993), Richards et al. (1998), and Fomalont et al. (2002) each required hundreds of hours of integration over a single VLA beam to detect a reasonable number of sources.

Since we do have well-determined source counts at mJy sensitivities *and below* at 8.5 GHz, it is of interest to try to determine the 8.5 GHz source counts at larger fluxes than this limit. The 10 GHz work of Aizu et al. (1987) provides source counts at $S > 100$ mJy, but these counts were determined by observing sources already measured at lower frequencies, as noted, and may therefore be underestimates of the true source counts at 10 GHz. Thus, there existed prior to this work a substantial gap in the 8.5 GHz source counts between roughly 0.3 and 100 mJy. Unfortunately, this is the flux density range of particular interest in source counts; in this range, the slope of the source count is expected to change because of the emergence of new classes of sources (see e.g., Windhorst et al. 1985; Condon 1992; Windhorst 2003).

This paper reports an attempt to fill this gap and to complete the source counts at 8.5 GHz. We used a combination of archival data and a few relatively brief blind surveys of the sky to obtain source counts at 8.5 GHz from $\sim$0.1 to $\sim$50 mJy. The use of archival data parallels the earlier methods and work at 4.8 GHz by Wrobel & Krause (1990).

Section 2 of this paper describes the procedures followed for analyzing both the archival data and our own survey data. We then go on in § 3 to derive the source counts and to compare them with previous results. Our results are briefly discussed in § 4.

2. PROCEDURE

2.1. *Archival Data*

Our aim was to reach a 4–5 σ detection level of 0.2 mJy or better at 8.5 GHz. At the VLA, an integrating time of at least 15 minutes would be required for each field to reach this level. In addition, the sensitivity of VLA images drops as distance r from the phase center of the field increases (dropping to 1/2 at $r = 2\farcm6$). On the other hand, to obtain a statistically significant sample of sources at mJy levels, given rough estimates of the source counts, we would need to form many VLA images. It seemed prohibitive to request the implied amount of observing time from the VLA. Instead, following Wrobel & Krause (1990), we made use of deep 8.5 GHz images made by other observers for other purposes. For this enterprise we needed relatively deep VLA images, but *without* a strong source present, since this would have limited the dynamic range of the images. Searches for radio emission from Galactic stars, especially if at high Galactic latitude, and deep searches for radio afterglows from gamma-ray bursts fulfilled both criteria nicely. In most cases the object sought was quite faint and hence presented no problems with the dynamic range of the images. In addition, images (or raw data) with a range of observing time were available in the VLA public archives.

Most of the archival data we used were taken from the work of S. Drake (2003, private communication) or of D. Frail (2003, private communication) and his collaborators, with their permission. In some cases the observers provided us with images that we used directly. In other cases, we obtained permission to use raw u-v data and imaged them ourselves using standard programs in AIPS. We then examined the images and noted sources with peak flux exceeding 5 times the rms noise of that image (7 σ in the case of images supplied by Drake, which had been lightly cleaned). The integrated sky flux densities, corrected for the primary beam response and other instrumental effects, were obtained with standard programs in AIPS. A description of this archival material is contained in Table 1, and the sources derived from it are cataloged in Table 2.

TABLE 1
ARCHIVAL DATA AT 8.5 GHz

Origin	Target Sources	Number of Serendipitous Sources	Average rms Noise (μJy beam^{-1})	VLA Configuration
Drake.....	Galactic stars	7	$\sim$30	Various
Frail.....	Gamma-ray bursts	7	$\sim$5	C
Guerra.....	GPS sources	2	$\sim$500	D or C/D

At the bright end of the flux density gap we were trying to fill, we also used some material obtained to support the work of Guerra, Cabanela, and Partridge on potential gigahertz-peaked spectrum (GPS) sources (see, e.g., Partridge et al. 2003). These were snapshot images at 8.5 GHz (and other frequencies) designed to make simultaneous, multifrequency observations of potential GPS or inverted spectrum sources. While the 5 σ threshold of these images was quite high, given the brief integration time, 16 were available, providing nearly 0.2 deg^2 of sky coverage. That enabled us to determine fluxes of a few 8.5 GHz sources detected serendipitously. We did not, of course, include the target sources themselves in our counts (but see § 3.1 below).

2.2. *Blind Survey at* 8.5 GHz

When we assembled the archival material, we discovered that we had found fewer sources than we had hoped, and there continued to be a gap in the source counts in the approximate flux density range 3–50 mJy. We therefore arranged to make shallow, wide-area surveys of two regions of the sky at 8.5 GHz. These two surveys were inserted during bad weather in the midst of another VLA observing program carried out in the spring of 2003, with the VLA in its D configuration. We calculated both the integrating time and the solid angle surveyed to match our target range of 3–50 mJy. The surveys were designed to have a 5 σ detection sensitivity at the X band of approximately 1 mJy and to cover a sufficiently large area to give us dozens of sources in the flux density range 3–50 mJy.

2.2.1. *Regions Surveyed*

The first area chosen for study was the Hubble Deep Field–North (HDF-N) and its flanking fields, because this area had been extensively surveyed at a wide range of wavelengths, and we had some 1.4 GHz flux densities available from the work of Richards (2000). The second area covered was a portion of the area surveyed by the CBI instrument to detect CMB fluctuations. After discussions with T. Pearson (2005, private communication), who had conducted a very shallow 8.5 GHz survey (as yet unpublished) centered at $8^{\rm h}$ and -3° to search for sources that might contribute foreground noise to CMB observations, we decided to resurvey a portion of that field at somewhat greater sensitivity. Since our survey was carried out in the winter of 2003, $\sim$30 months after the bulk of the observations by Pearson and his colleagues, we also can investigate the variability of the sources we both detected at 8.5 GHz once the CBI-related survey is available.

Our blind surveys were made in a raster pattern, one centered on the HDF at $12^{\rm h}36^{\rm m}49^{\rm s}$ and $+62^\circ13'00''$ and a narrower

TABLE 2
SOURCES AT 8.5 GHz

Source (1)	Origin[a] (2)	R. A. (J2000.0) (3)	Decl. (J2000.0) (4)	Corrected Flux S (mJy) (5)	Effective Area (sr) (6)
1	Frail	03 42 42.21	17 11 05.6	0.0822 ± 0.0115	2.17E−06
2	Frail	03 42 15.93	17 09 42.0	0.576 ± 0.012	1.00E−05
3	Frail	23 29 48.55	−23 54 41.4	0.312 ± 0.052	8.65E−06
4	Frail	23 29 40.00	−23 52 54.7	0.419 ± 0.027	1.06E−05
5	Frail	23 29 33.11	−23 51 28.4	2.81± 0.09	5.23E−05
6	Frail	23 29 30.77	−23 53 06.7	0.334 ± 0.028	1.01E−05
7	Frail	23 29 27.09	−23 56 48.8	0.0963 ± 0.0275	6.83E−06
8	Guerra	02 20 27.54	01 14 01.8	17.25 ± 1.59	1.30E−04
9	Guerra	07 09 46.08	49 45 53.0	5.19 ± 0.99	1.12E−04
10	Drake	17 47 05.30	05 37 15.0	4.82 ± 0.08	1.18E−04
11	Drake	18 42 44.60	55 29 22.0	1.30 ± 0.04	6.69E−05
12	Drake	18 42 54.00	55 35 26.0	5.85 ± 0.04	1.23E−04
13	Drake	19 05 44.60	−15 42 19.0	4.07 ± 0.12	7.35E−05
14	Drake	19 59 35.50	−34 44 46.0	2.73 ± 0.05	9.78E−05
15	Drake	20 00 08.60	−34 39 48.0	6.73 ± 0.10	1.15E−04
16	Drake	09 07 39.50	10 42 43.0	1.89 ± 0.09	8.13E−05
17	2003 Feb 20	12 33 36.53	62 30 20.7	13.11 ± 0.85	2.06E−04
18[b]	2003 Feb 20	12 34 11.96	61 58 31.1	7.36 ± 3.59	2.06E−04
19	2003 Feb 20	12 34 52.16	62 02 36.5	52.27 ± 2.48	2.06E−04
20	2003 Feb 20	12 35 38.16	62 19 32.5	12.10 ± 1.31	2.06E−04
21	2003 Feb 20	12 35 50.87	62 27 58.9	3.09 ± 0.99	9.53E−05
22[b]	2003 Feb 20	12 36 55.62	61 57 09.4	11.82 ± 4.70	1.49E−04
23[b]	2003 Feb 20	12 39 16.45	62 00 17.0	17.61 ± 2.67	2.06E−04
24	2003 Feb 20	12 39 39.44	62 01 25.7	27.78 ± 3.02	2.06E−04
25	2003 Feb 20	12 39 41.69	62 32 05.9	3.85 ± 1.69	5.77E−05
26	2003 Feb 20	12 39 53.71	62 21 13.7	2.76 ± 1.31	5.57E−05
27	2003 Feb 20	12 40 12.02	62 26 32.1	4.60 ± 0.94	1.57E−04
28	2003 Feb 27	08 46 13.24	−03 26 19.8	9.30 ± 0.63	2.35E−04
29	2003 Feb 27	08 46 29.78	−03 25 02.0	2.73 ± 0.69	1.64E−04
30	2003 Feb 27	08 47 11.73	−03 23 00.5	8.35 ± 0.53	2.35E−04
31	2003 Feb 27	08 48 34.36	−03 21 04.2	2.37 ± 0.65	1.82E−04
32	2003 Feb 27	08 48 55.86	−03 24 50.7	4.07 ± 0.68	2.35E−04
33	2003 Feb 27	08 49 44.69	−03 17 56.9	63.00 ± 0.67	2.35E−04
34	2003 Feb 27	08 50 41.69	−03 23 09.9	1.92 ± 0.69	1.53E−04
35	2003 Feb 27	08 52 37.85	−03 24 50.7	3.86 ± 0.78	2.35E−04
36	2003 Feb 27	08 52 44.26	−03 22 39.8	4.90 ± 0.84	2.35E−04
37[c]	2003 Feb 27	08 54 02.30	−03 19 17.8	1.37 ± 0.55	1.14E−04
38	2003 Feb 27	08 54 09.31	−03 23 31.4	22.60 ± 0.59	2.35E−04
39	2003 Mar 15	12 34 09.02	62 39 54.0	4.73 ± 0.48	2.35E−04
40	2003 Mar 15	12 35 19.32	61 48 16.5	1.80 ± 0.83	3.06E−05
41	2003 Mar 15	12 35 54.69	61 48 03.5	42.53 ± 1.33	2.35E−04
42	2003 Mar 15	12 36 41.34	62 40 06.0	8.51 ± 0.51	2.35E−04
43	2003 Mar 15	12 37 29.20	61 44 53.8	10.53 ± 2.81	1.30E−04
44[c]	2003 Mar 15	12 38 56.19	62 43 10.0	3.02 ± 0.83	1.20E−04
45[c]	2003 Mar 15	12 39 39.38	62 43 07.2	2.69 ± 0.78	9.63E−05
46	2003 Mar 15	12 39 46.41	62 37 17.0	1.81 ± 0.59	1.25E−04
47	2003 Mar 15	12 39 57.53	61 48 27.2	3.28 ± 0.76	1.20E−04

NOTE.—Units of right ascension are hours, minutes, and seconds, and units of declination are degrees, arcminutes, and arcseconds.

[a] Archival sources are identified by the name of the author who originally made the observations. Blind survey sources are identified by the date observed.

[b] Sources detected below 5 σ at 8.5 GHz, in particularly noisy images.

[c] Sources detected above 5 σ at 8.5 GHz and found in the FIRST catalog, but with no obvious 4.8 GHz counterpart.

east-west strip centered at $08^{h}50^{m}05^{s}$ and $-03^{\circ}22'00''$, both in J2000.0 coordinates. Separate pointings spaced by 4.′9 or $\sim$2 beam widths were combined to produce a mosaic of each strip. The scan pattern for the HDF region is illustrated in Figure 1. The solid angles of the two strips were 3.138×10^{-4} and 1.279×10^{-4} sr, respectively. The integration time per pointing, 40 s, was chosen to give reliable $\sim$5 σ detections down to $\sim$1 mJy at the beam center. Since each image has a useful radius of $\sim$4.′5, significant overlapping occurred within both fields. This allowed us to align the images and to confirm marginally detected sources. However, it introduced complications when determining differential source counts, so we present in § 3 a method for dealing with this problem.

Standard NRAO data reduction procedures in AIPS were used to form and clean the individual images in each mosaic. Calibration was based on VLA calibrator 1331+305 (3C 286), for which

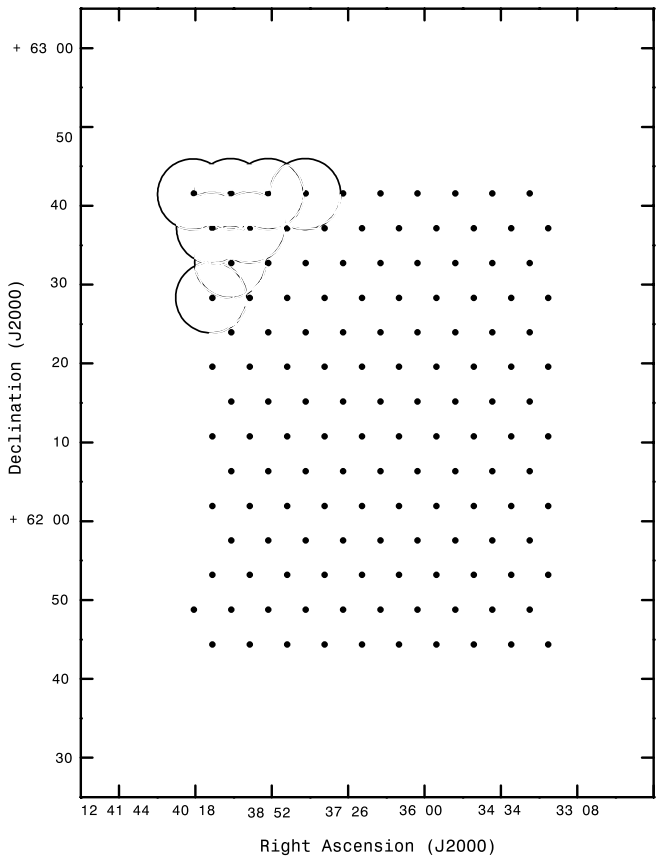

FIG. 1.—Area covered in the HDF blind survey. Corresponding 4.′5 radius map areas are shown for just a few pointings. Similarly spaced pointings were used for the 8^h field, but along a narrow strip at $-03^\circ 22'$.

we assumed a 8.5 GHz flux density of 5.20 Jy. For the 8.5 GHz images, we used 2″ pixels and relatively light cleaning to reduce sidelobe effects. In a few images in which relatively bright sources appear (e.g., the double-lobed source at $12^h35^m55^s$ and $+61^\circ 48' 04''$ with $S \sim 43$ mJy), we cleaned the image more deeply in a box centered on the bright source.

Because the observations were made in periods of poor weather (rain, wet snow, and/or ice), particularly on February 20, the resulting rms noise in the image was often higher than expected from receiver noise alone. Typical values of the rms for the three observing runs were $\sigma = 430$ (February 20), 185 (February 27; the 8^h field), and 135 μJy (March 15). There was also variation from field to field within each day's run. For instance, the rms noise of images formed on March 15 varied from 125 to 160 μJy. In the case of the very noisy February 20 data, images that included real sources were further cleaned just around those sources with between 50 and 100 iterations. This allowed us to determine more accurately the fluxes for these sources and bring down the rms noise to a reasonable level. This additional step of cleaning typically reduced the rms noise of the image to $\sim$90% of its previous value. For the purpose of calculating effective area, the rms noise values for blank fields were also scaled down to $\sim$90% of their original value based on these findings. It was necessary to clean more aggressively *after* the sources were identified to avoid counting overcleaned artifacts or spikes in the noise as real sources.

The two blind surveys covered a total area of about 1.5 deg^2 and yielded a total of 31 secure 8.5 GHz detections. The details for these sources appear in Table 2.

2.2.2. *Multifrequency Observations*

In both fields of our blind survey, we made supporting observations to approximately the same sensitivity at a lower frequency, 4.8 GHz. These observations allowed us to determine rough spectral indices for the sources detected and had the further advantage of providing a check on our 8.5 GHz detections; we felt confident accepting 4 σ detections at 8.5 GHz if there was a 4.8 GHz source at the same position. Recall that we also had some 1.4 GHz fluxes available from earlier surveys in the HDF-N region. In addition, our brighter sources appeared in earlier large-area 1.4 GHz surveys such as NVSS (NRAO VLA Sky Survey; Condon et al. 1998) or FIRST (Faint Images of the Radio Sky at Twenty cm; Becker et al. 1995). These allow us to calculate 1.4–4.8 GHz spectral indices as well. The spectral indices are shown in Table 3; the mean 4.8–8.5 GHz spectral index is $\alpha = 0.51$ ($\nu^{-\alpha}$). Given the large scatter in the spectral indices, we also give the median and quartile values. These are $\alpha = 0.63$, and 0.13 and 1.05, respectively, for the 4.8–8.5 GHz spectral index.

The 4.8 GHz mosaic was constructed with 8.′5 beam spacings, with an integration time of 60 s per pointing. The data were calibrated, imaged, and cleaned in the same fashion as the 8.5 GHz data, with a pixel size of 3″. Typical values of the rms were 220 (February 27) and 160 μJy (March 15); no 4.8 GHz data were taken on February 20. The lower frequency surveys completely covered the two strips mosaicked at 8.5 GHz.

2.2.3. *Finding Sources in the Blind Survey Areas*

Each 8.5 GHz (or 4.8 GHz) image was searched for potential sources with peak flux exceeding 5 σ, where σ was the rms noise measured in that image. The search was restricted to a circle of radius 4.′5 (or $\sim$8′ at 4.8 GHz); at that value of r, the primary beam response of the VLA has fallen to $\sim$0.086. Potential sources that appeared in more than one pointing in a mosaic were counted if their flux exceeded 5 σ in either image.

Next, the 4.8 GHz images were searched at the position of each potential 8.5 GHz source. Any source with peak flux $S > 5\ \sigma$ at 8.5 GHz *and* a corresponding detection >5 σ in the 4.8 GHz image was included in our counts. Positional agreement within half the FWHM of the 8.5 GHz restoring beam ($\sim$5″) was required for correspondence between the two frequencies. Marginal detections above 5 σ at 8.5 GHz were also investigated for correspondence in the 4.8 GHz images down to 4 σ, but no new 4.8 GHz sources were identified this way. Finally, for every source seen at >5 σ in the 4.8 GHz images, we returned to the higher frequency 8.5 GHz images to look for indications of the same source with peak flux down to 4 σ at 8.5 GHz. In three cases (numbers 18, 22, and 23) we found weak 8.5 GHz sources within 2–3 pixels of the positions of 4.8 GHz sources; these too were included in our counts, but flagged. One of these cases, source 23, is very securely detected at 8.5 GHz; its *integrated* flux is $\sim$7 times the associated error in flux. On the other hand, for seven reliable (>5 σ) detections at 4.8 GHz, no sources >4 σ were visible at 8.5 GHz. These sources presumably had spectral indices steeper than $\sim$1.2. In two cases, where the 8.5 GHz observations were made a month before the corresponding 4.8 GHz measurements, variability could have played a role.

Since many of our sources were bright enough to appear in wide-area 1.4 GHz surveys such as NVSS (Condon et al. 1998) and FIRST (Becker et al. 1995), we had an additional way to confirm the reality of our 8.5 GHz sources. Three potential 8.5 GHz sources (37, 44, and 45) that had no obvious counterparts at 4.8 GHz did, however, match the position of a FIRST source to $\lesssim$10″. They were also included in our counts, but again flagged.

TABLE 3
SPECTRAL INDICES FOR SHALLOW SURVEY SOURCES

Source	8.5 GHz Flux (mJy)	4.8 GHz Flux (mJy)	Spectral Index α[a] (8.5–4.8 GHz)	1.4 GHz Flux (mJy)	Spectral Index α (4.8–1.4 GHz)
17	13.11 ± 0.85	16.80 ± 1.00	0.45	38.19	0.66
18	7.36 ± 3.59	14.04 ± 0.74	1.17	23.96	0.43
19	52.27 ± 2.48	78.37 ± 0.82	0.73	244.51	0.91
20	12.10 ± 1.31	20.79 ± 0.60	0.98	65.68	0.92
21[b]	3.09 ± 0.99	7.82 ± 0.64	1.68	10.51	0.24
22	11.82 ± 4.70	12.71 ± 1.09	0.13	28.0[c]	0.63
23	17.61 ± 2.67	10.08 ± 1.11	−1.01	28.8[c]	0.84
24	27.78 ± 3.02	9.75 ± 1.03	−1.89	...	...
25	3.85 ± 1.69	15.64 ± 3.07	2.53	15.61	0.00
26	2.76 ± 1.31	5.44 ± 1.43	1.22	8.59	0.37
27[b]	4.60 ± 0.94	43.23 ± 1.69	4.04	258.71	0.95
28	9.30 ± 0.63	8.75 ± 0.53	−0.11	...	...
29	2.73 ± 0.69	2.43 ± 0.44	−0.21	7.9	0.95
30	8.35 ± 0.53	11.86 ± 0.62	0.63	21.25	0.47
31	2.37 ± 0.65	4.24 ± 0.66	1.05	8.66	0.57
32	4.07 ± 0.68	4.15 ± 0.75	0.04	3.47	−0.14
33	63.00 ± 0.67	68.52 ± 0.77	0.15	76.19	0.09
34	1.92 ± 0.69	2.82 ± 0.78	0.69	...	...
35	3.86 ± 0.78	4.83 ± 0.68	0.40	2.97	−0.39
36	4.90 ± 0.84	2.21 ± 0.60	−1.44	...	...
37	1.37 ± 0.55	...	...	5.29	...
38	22.60 ± 0.59	53.75 ± 0.85	1.56	123.89	0.67
39	4.73 ± 0.48	8.26 ± 0.43	1.01	23.02	0.82
40	1.80 ± 0.83	2.05 ± 0.91	0.23	4.5[c]	0.63
41[b]	42.53 ± 1.33	89.83 ± 1.46	1.35	261.14	0.86
42	8.51 ± 0.51	11.07 ± 0.54	0.47	23.49	0.60
43[b]	10.53 ± 2.81	14.27 ± 1.34	0.55	25.9[c]	0.48
44	3.02 ± 0.83	...	...	3.6	...
45	2.69 ± 0.78	...	...	2.76	...
46	1.81 ± 0.59	2.63 ± 0.64	0.67	4.25	0.39
47	3.28 ± 0.76	5.17 ± 0.69	0.82	11.7[c]	0.66

[a] The spectral index was determined using the $\nu^{-\alpha}$ convention.
[b] See § 2.2.4 for comments on these sources.
[c] Fluxes are from NVSS. All other 1.4 GHz fluxes are from FIRST.

2.2.4. *Source Fluxes*

Once a source had been detected as described above, we determined its true flux density by correcting for the primary beam response of the VLA, then fitting an elliptical Gaussian profile to the source and obtaining its integrated flux density. These operations were performed with standard routines (PBCOR and JMFIT) in the AIPS software package. The latter program produces error estimates for the integrated flux density of sources, including uncertainties in fitting the profile. These are the errors listed in column (5) of Table 2. In some cases, these errors exceed 1/5 of the flux density (even though the peak flux density of the source exceeded 5 times the rms noise of the image). We included these sources in our counts because (1) they met the 5 σ threshold criterion and (2) in every case a corresponding source was seen either in our 4.8 GHz survey, the FIRST survey, or both. Thus, we believe that these sources (such as numbers 37 and 45) are real and should be included in our counts. On the other hand, the flux density of these weak sources may be slightly overestimated as a consequence of a bias discussed by Hogg & Turner (1998). In our work, the signal-to-noise ratio for all sources exceeds 5, and the slope of the (integral) source counts is close to −1. Using these values in equation (4) of Hogg & Turner, we find that the correction to the flux densities even in the case of our weakest sources is $\leq$10%. We have elected not to make these small corrections to the flux densities of the weakest sources, given the much larger uncertainties in our source counts.

Two sources, 41 and 43, were clearly multiple. In these cases, we summed the flux density from the two or three components of each source and treated each of the extended objects as a single entry in the source counts. In addition, source 27 was a clear double and resolved in our 4.8 GHz image, but only one of the two components was (marginally) visible at 8.5 GHz. In calculating the 4.8–8.5 GHz spectral index, we compared 8.5 and 4.8 GHz flux densities of that component only. Even so, the spectral index (4.04) is suspicious, probably because some of the higher frequency flux was resolved out (see § 3.2 below), and we did not include this source when calculating mean spectral indices. On the other hand, to compare the 4.8 GHz flux density with the FIRST results, we added the 4.8 GHz flux density of both components, giving 79.79 ± 3.02 and a (more reasonable) 1.4–4.8 GHz spectral index of 0.95. Source 21 may also have lost flux as a result of resolution at 8.5 GHz.

3. SOURCE COUNTS AND THE 8.5 GHz log N–log S DIAGRAM

The composite of the 8.5 GHz source count data was separated into three different groups, as shown in Table 4, before the differential source count was determined. The archival sources were kept separate from the blind survey sources, because the archival data were not homogeneous. The blind survey sources were divided into two groups, one containing sources from the February 27 and March 15 observations and the other containing

TABLE 4
SOURCE COUNTS AT 8.5 GHz

Data Set	Flux Density Interval (mJy)	Weighted Flux $\bar{S}$ (mJy)	Number[b]	n (sr^{-1})	$(\bar{S})^{5/2}dN/dS$ (sr^{-1} $Jy^{1.5}$)
Archival	0.08–0.84	0.21	6	1015354	0.834
	0.84–5.00	1.80	6.6	84344	2.787
	5.00–20.00	9.24	4.7	38296	20.953
Blind Survey[a] 2003 Feb 20	2.73–4.20	3.36	3	45766	20.374
	4.20–12.60	6.92	4	22784	10.809
	12.60–55.00	24.09	4	19413	41.222
Blind Survey 2003 Feb 27, 2003 Mar 15	1.35–3.15	2.00	8	87486	8.716
	3.15–6.32	4.37	5	25375	10.123
	6.32–30.50	12.55	5	24730	18.039
	30.50–70.00	44.90	2	8507	92.022

[a] Survey made in extremely poor weather.
[b] The unweighted number of sources found within the flux limits of each bin.

sources from the February 20 observations taken in extremely poor weather. This latter split was necessary because of the significantly higher rms noise values in the February 20 data.

Each group of sources was binned by intervals of flux density, and we followed the methods of Condon et al. (1982) to calculate the weighted number of sources per steradian, n, for each bin. This is given by

$$n = \sum_{i=1}^{N} \Omega_i^{-1},$$

where Ω_i is the area in which the ith source could have been detected above the 5 σ (or other) threshold in the relevant image. From here on, Ω_i is referred to as the "effective area." We similarly calculated the rms statistical error in n as

$$\sigma = \left(\sum_{i=1}^{N} \Omega_i^{-2} \right)^{1/2}.$$

The effective area calculated in this way for bright sources in the blind survey was often greater than the entire area we surveyed. These were sources bright enough to have been seen anywhere in the survey. To remedy this situation, we set the maximum effective area for each source to the entire size of the relevant survey (e.g., 2.06×10^{-4} sr for February 20). This did not prevent all potential overlapping of effective areas within the fields, since rms noise values vary from map to map, but it does properly set the effective source count of these bright sources to unity. For three additional relatively bright sources it was necessary to calculate a correction for the overlap of effective areas (typically $\sim$10%), and we did so. The remaining sources were so faint that they could be detected only near the phase centers of the images, so that overlap was not an issue.

The calculated number of sources per steradian (n) was divided by the width of each flux density interval expressed in janskys and then divided by a properly weighted average flux density $\bar{S}^{-2.5}$ to obtain the normalized differential source count $S^{2.5}(dN/dS)$ expressed in units of $Jy^{1.5}$ sr^{-1}. The parameter $\bar{S}$ was determined for each bin as

$$\bar{S} = \frac{\int_{S_l}^{S_u} S(dN/dS)\, dS}{\int_{S_l}^{S_u} (dN/dS)\, dS},$$

where S_u and S_l are the upper and lower limits of the flux density bin, respectively. In the range of flux densities of interest, our counts suggest that dN/dS scales roughly as S^{-2}; hence, the index -2 was used in evaluating these integrals.

3.1. *Including Central, Targeted Sources in the Archival Data*

It is reasonable to consider including in our count a certain fraction of the target sources from the archival search, since in a completely blind survey there would be some probability of finding such sources in the field. The target sources in the data supplied by D. Frail (2003, private communication) and S. Drake (2003, private communication) were gamma-ray bursts and stars, respectively, so they were not included, since our interest is in extragalactic radio sources and not Galactic objects or transient phenomena. The 8.5 GHz snapshot observations of potential GPS sources (see Partridge et al. 2003), on the other hand, *were* centered on extragalactic radio sources. These ranged in flux density from $\sim$3 to 170 mJy; 16 images were used. In these, as noted, we found two serendipitous sources. To estimate the probability that one of the *target* sources would have been found in a truly blind survey, we repeated effective area calculations for each target source and combined these results with the $\log N$–$\log S$ relation derived from our counts. The probability of detecting one 3 mJy source in these 16 images was $\sim$60%. We therefore added to our direct count of sources in the 0.84–5.0 mJy bin 0.6 "sources" at 3 mJy. Similar calculations added 0.3 "sources" at 11.5 mJy and 0.4 at 18 mJy to the 5–20 mJy bin. In this way, we took account of the fact that a few sources similar in flux density to those we specifically targeted in our work on potential GPS objects might have been found in a truly blind survey. To check these results, we calculated, using our own source counts, the number of sources with 8.5 GHz flux density $\geq$3 mJy we would have expected in a truly blind survey covering the area of the GPS work (16 images). The answer is 2.4, in reasonable agreement with our corrected "counts" of 3.3.

3.2. *Completeness and Corrections for Resolved Sources*

We now consider issues related to the *completeness* of our list of sources and to the possibility that we missed sources because their angular size substantially exceeded the synthesized beam of the VLA, so that their true flux was not measured.

The list of sources we report in Table 3 is certainly not a complete list of all sources in our search areas exceeding the threshold of our blind survey (roughly 1 mJy). The response of the VLA varies across the primary beam and hence across the

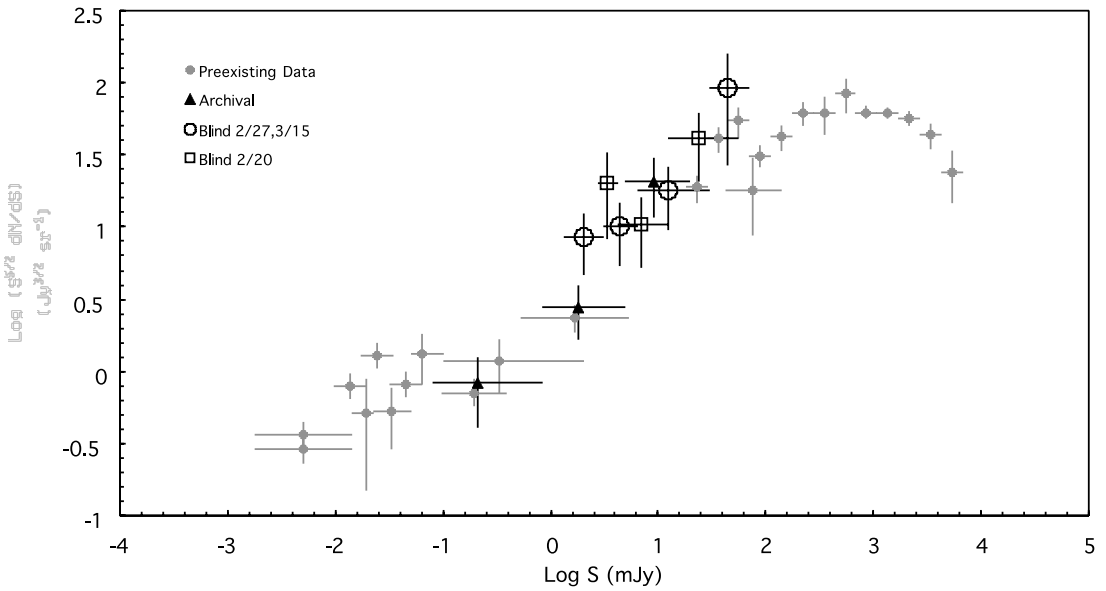

FIG. 2.—Source counts at 8.5 GHz including our new data points.

area surveyed. Thus, for instance, a 1.5 mJy source would exceed our threshold and be counted if it fell near the phase center of one of our VLA images, but not if it fell more than $\sim 2'$ distant from the phase center. Table 3 is a complete list of sources in this sense only for values of flux density $S \gtrsim 4-7$ mJy, depending on the date of observation. On the other hand, the *counts* we report are correct; the effective area calculation discussed earlier in this section properly takes account of the primary beam response of the VLA.

The same statement can be made about the archival counts—they are by no means *complete*, but the *counts* are correct.

Next, there is the issue of resolution. If a source is substantially larger than the synthesized beam of the VLA, its true flux is not recorded by the instrument. In particular, the peak flux recorded may fall below our 5 σ detection threshold, so that we miss the source entirely, even though its true integrated flux may be substantial. Clearly, the undercount is likely to be worse for extended sources whose integrated flux lies near our detection threshold. To examine the possibility of an undercount due to resolution effects, we need to know the angular size distribution of $\sim$1 mJy sources at 8.5 GHz. The work of Windhorst et al. (1993) suggests that roughly 20% of all 8.5 GHz sources have an angular scale exceeding the $6''$ scale of the synthesized beam used in our blind surveys. Thus, our counts in the lowest flux density bins for the two blind surveys could undercount sources by as much as 20%. However, more recent work, albeit at 1.4 GHz, suggests a much smaller proportion of extended sources. Fomalont et al. (2005), for instance, find that only 4% of individual sources in a deep 1.4 GHz survey exceed $4''$ in scale and argue that many of the extended ($>4''$) sources reported in other surveys are blends of two or more discrete objects. Countering this, Garrett et al. (2000) in another deep 1.4 GHz survey with $\sim 10''$ resolution *do* find extended sources missed by earlier VLA surveys of the same region. In view of the uncertainty in the angular size distribution, we have elected *not* to make any correction for a possible undercount due to resolution effects. The magnitude of a possible undercount ($\sim$4%–20%) in any case is less than or comparable to our statistical errors in the blind survey counts.

The issue of resolution is more complicated when we consider the archival data. In the case of the images obtained from Drake and Frail, the synthesized beam was smaller than the $\sim 6''$ used for our blind survey. We employed a 7 σ detection threshold for the Drake data to help mitigate this problem. In the case of the Guerra data, the VLA was in its most compact D configuration or in a hybrid C/D configuration, so the synthesized beam was again $\sim 6''$.

Our final normalized differential source counts are shown in Figure 2. This figure also shows earlier 8.5 and 10 GHz source counts from the literature, as described in § 1.

4. DISCUSSION

The general shape of the normalized $\log N$–$\log S$ curve of Figure 2 resembles that seen at lower frequencies; we see no surprises. We do now have data on the source counts at values of the flux density where a new population of sources begins to emerge, flattening the slope of the $\log N$–$\log S$ curve (see, for instance, the models of Toffolatti et al. 1998 or De Zotti et al. 2005). That transition in our data occurs at $S \sim 1$ mJy.

4.1. *Comparison to Source Counts at Lower Frequencies*

We now compare the 8.5 GHz counts derived from both our results and the literature (Fig. 2) with the counts at the next lowest frequency for which extensive source counts are available, 4.8 GHz (Gregory & Condon 1991; see also summary in Windhorst et al. 1993). There are essentially no qualitative differences. A quantitative comparison of our counts in the 0.1–30 mJy range with the 4.8 GHz counts shown by Windhorst et al. (1993) shows that only a small offset is required to align the counts. At any given flux density in that range of S, there are only $\sim$30% more 4.8 GHz sources than 8.5 GHz sources per unit area. This finding in turn suggests that the typical 8.5–4.8 GHz spectral index of 0.1–30 mJy sources must be small, in qualitative agreement with both the findings of Windhorst et al. (1993), who find $\bar{\alpha} = +0.35 \pm 0.15$ for sources in the flux density range we explore, and our mean value of +0.51.

4.2. *Comparison to Source Counts at Higher Frequencies*

As noted in § 1, counts over limited regions of the sky at frequencies higher than 8.5 GHz are now becoming available, and

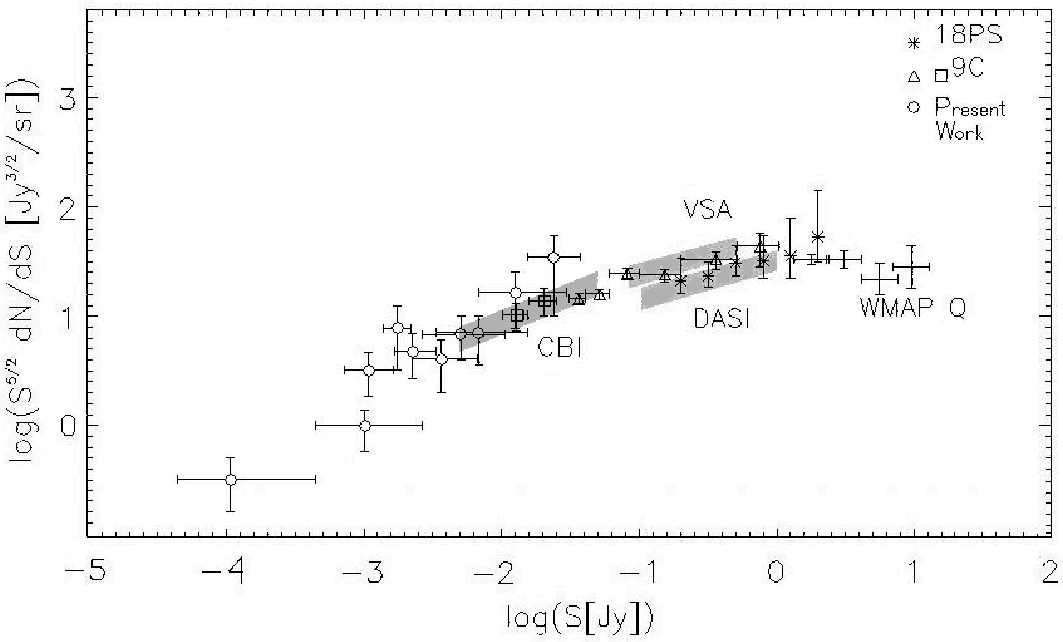

FIG. 3.—Comparison of our source counts, scaled to 30 GHz as explained in the text, with counts at higher flux densities made in the 15–30 GHz range.

WMAP has just performed an all sky-survey in several frequency bands from 22 to 90 GHz. The *WMAP* paper by Bennett et al. (2003) includes a graph comparing many of these higher frequency source counts (see that paper for references). A variant of that figure constructed by R. Ricci (2005, private communication) is reproduced above, with two additions of surveys not available to Bennett et al.: first, the 15 GHz counts of the 9C survey, and second, the 18 GHz source counts from the ATCA southern survey of Ricci et al. (2004). Most of the source counts shown in Figure 3 were made at frequencies of roughly 15–30 GHz. To compare our source counts fairly, some adjustment depending on the spectral index of sources between 8.5 and 15–30 GHz is required. That is, if we assume that exactly the *same* sources are contributing to our counts and to the 30 GHz counts, we need to scale both S and N appropriately. The scaling factor in flux density is $(30/8.5)^{-\alpha}$, and the corresponding adjustment in N is $(30/8.5)^{-3\alpha/2}$. For the spectral index α we take $+0.5$, based on the average α derived from our own 8.5 and 4.8 GHz measurements. We simply assume, in the absence of hard data, that α stays constant from 8.5 to 30 GHz. With those corrections, our source counts fall as shown in Figure 3.

Three qualitative features emerge from this comparison. First, the overall fit is reasonably good to the CBI and 9C counts, as shown in Figure 3, as well as to the Toffolatti et al. (1998) models. There are no surprises here, as well. Second, our (scaled) counts at flux densities $\gtrsim$10 mJy lie slightly above the 9C counts, as well as the counts predicted by the models of Toffolatti et al. (1998). That, in turn, suggests that there is no substantial population of high-frequency sources *not* seen at 8.5 GHz. The excess in (scaled) 8.5 GHz counts at $S \gtrsim 10$ mJy may be due to an admixture of steep-spectrum sources that drop out of the 15–30 GHz source counts (if we had adopted $\alpha = 0.7$, say, instead of $\alpha = 0.5$ in scaling our counts to 30 GHz, our results would match the 9C counts better). These results are encouraging for the *Planck* mission; our results combined with direct counts at $\sim$30 GHz show no evidence for a population of high-frequency sources hidden at 8.5 GHz in the flux density range likely to produce foreground noise in *Planck* CMB images. Next, our (scaled) counts fall slightly below Toffolatti's models at low flux density ($S \lesssim 1$ mJy). This may indicate that the value of α we used to scale our 8.5 GHz counts is too steep (at 0.5) at these low values of S. Finally, the slope of our counts in the normalized $\log N - \log S$ plot is steeper in the range 0.1–30 mJy than Toffolatti's models suggest or than the CBI counts. This could be explained by a gradual flattening of the spectral index α as S decreases from 30 to 0.1 mJy or by a tail of faint steep-spectrum sources that appear at 8.5 GHz but are below catalog limits at $\sim$30 GHz.

We end by reemphasizing that the general agreement of our (scaled) counts and those at $\sim$30 GHz shows no evidence for the emergence of a new population of high-frequency sources.

This research was supported principally by NSF grant AST 00-71192 to Haverford College. Additional funds to support undergraduate student involvement came from the Keck Northeast Astronomy Consortium. Several Haverford College undergraduates were involved in early phases of this work; these include Ben Seelig, Owen Newkirk, and Megan Roscioli. In addition, a summer research student from Colgate University, Michele Caler, was also involved in the analysis of some of the archival data; she was supported by Keck Northeast Astronomy Consortium funds.

We want to thank in particular the colleagues who provided data for our archival search, Steve Drake and Dale Frail. We would also like to thank Joan Wrobel and Tim Pearson for providing some early advice and several colleagues including Luigi Toffolatti for helpful comments on a draft of this work. Finally, the report of an anonymous referee on the first version of this paper was particularly detailed and helpful.

REFERENCES

Aizu, K., Inoue, M., Tabara, H., & Kato, T. 1987 in IAU Symp. 124, Observational Cosmology, ed. A. Hewitt, G. Burbidge, & L. Z. Fang (Dordrecht: Reidel), 565
Becker, R. H., White, R. L., & Helfand, D. J. 1995, ApJ, 450, 559
Bennett, C., et al. 2003, ApJS, 148, 1
Condon, J. J. 1992, ARA&A, 30, 575
Condon, J. J., Condon, M. A., & Hazard, C. 1982, AJ, 87, 739
Condon, J. J., Cotton, W. D., Greisen, E. W., Yin, Q. F., Perley, R. A., Taylor, G. B., & Broderick, J. J. 1998, AJ, 115, 1693
Danese, L., Franceschini, A., Toffolatti, L., & de Zotti, G. 1987, ApJ, 318, L15
DeZotti, G., Ricci, R., Mesa, D., Silva, L., Mazzotta, P., Toffolatti, L., & González-Nuevo, J. 2005, A&A, 431, 893
Fomalont, E. B., Kellermann, K. I., Cowie, L. L., Capak, P., Barger, A. J, Partridge, R. B., Windhorst, R. A., & Richards, E. A. 2005, ApJS, submitted
Fomalont, E. B., Kellermann, K. I., Partridge, R. B., Windhorst, R. A., & Richards, E. A. 2002, AJ, 123, 2402
Fomalont, E. B., Kellermann, K. I., Richards, E. A., Windhorst, R. A., & Patridge, R. B. 1997, ApJ, 475, L5
Fomalont, E. B., Kellermann, K. I., Wall, J. V., & Weistrop, D. 1984, Science, 225, 23
Fomalont, E. B., Partridge, R. B., Lowenthal, J. D., & Windhorst, R. A. 1993, ApJ, 404, 8
Garrett, M. A., de Bruyn, A. G., Giroletti, M., Baan, W. A., & Schilizzi, R. T. 2000, A&A, 361, L41
Gregory, P. C., & Condon, J. J. 1991, ApJS, 75, 1011
Haarsma, D. B., Partridge, R. B., Windhorst, R. A., & Richards, E. A. 2000, ApJ, 544, 641
Hogg, D. W., & Turner, E. L. 1998, PASP, 110, 727
Jackson, C. A., & Wall, J. V. 1999, MNRAS, 304, 160
Jauncey, D. L. 1975, ARA&A, 13, 23
Kovac, J. M., Leitch, E. M., Pryke, C., Carlstrom, J. E., Halverson, N. W., & Holzapfel, W. L. 2002, Nature, 420, 772
Mason, B. S., et al. 2003, ApJ, 591, 540
Partridge, R. B., Cabanela, J. E., Myers, S., & Guerra, E. J. 2003, BAAS, 35, 724
Ricci, R., et al. 2004, MNRAS, 354, 305
Richards, E. A. 2000, ApJ, 533, 611
Richards, E. A., Kellermann, K. I., Fomalont, E. B., Windhorst, R. A., & Partridge, R. B. 1998, AJ, 116, 1039
Ryle, M. 1968, ARA&A, 6, 249
Toffolatti, L., Argueso Gomez, F., de Zotti, G., Mazzei, P., Franceschini, A., Danese, L., & Burigana, C. 1998, MNRAS, 297, 117
Vielva, P., Martínez-González, E., Gallegos, J. E., Toffolatti, L., & Sanz, J. L. 2003, MNRAS, 344, 89
Waldram, E. M., Pooley, G. G., Grainge, K. J. B., Jones, M. E., Saunders, R. D. E., Scott, P. F., & Taylor, A. C. 2003, MNRAS, 342, 915
Windhorst, R. A. 2003, NewA Rev., 47, 357
Windhorst, R. A., Fomalont, E. B., Partridge, R. B., & Lowenthal, J. D. 1993, ApJ, 405, 498
Windhorst, R. A., Miley, G. K., Owen, F. N., Kron, R. G., & Koo, D. C. 1985, ApJ, 289, 494
Wrobel, J. M., & Krause, S. W. 1990, ApJ, 363, 11